Low Complexity Concurrent Constant Modulus Algorithm and Soft Decision Directed Scheme for Blind Equalization

S. Chen

Department of Electronics and Computer Science
University of Southampton, Southampton SO17 1BJ, U.K.
Tel./Fax: +44 (0)23 8059 6660/4508
E-mail: sqc@ecs.soton.ac.uk

Abstract

The recently introduced concurrent constant modulus algorithm (CMA) and decision-directed (DD) scheme provides a state-of-art low-complexity blind equalization technique for high-order quadrature amplitude modulation (QAM) channels. At a small cost of slightly more than doubling the complexity of the standard CMA blind equalizer, this concurrent CMA and DD blind equalizer obtains a dramatical improvement in equalization performance over the CMA. In this paper, a new blind equalization scheme is proposed based on concurrent CMA and a novel soft decision-directed (SDD) adaptation. The proposed concurrent CMA and SDD blind equalizer has simpler computational requirements than the concurrent CMA and DD algorithm. Extensive simulation shows that it has the same steady-state equalization performance as the concurrent CMA and DD algorithm and a faster convergence speed over the latter scheme.

Keywords: Quadrature amplitude modulation, blind equalization, constant modulus algorithm, decision-directed adaptation, bootstrap maximum *a posteriori* probability.

1 Introduction

Blind equalization improves system bandwidth efficiency by avoiding the use of a training sequence. Furthermore, for certain communication systems, training is infeasible and blind equalizer provides a practical means for combating the detrimental effects of channel dispersion in such systems. For systems employing high bandwidth-efficiency quadrature amplitude modulation (QAM) signalling, the constant modulus algorithm (CMA) based equalizer [1]–[4] is by far the most popular low-complexity blind equalization scheme, as it can readily meet the real-time computational constraint. There has been many studies which investigate convergence behaviour of the CMA. A particular problem of the CMA is that its steady-state mean square error (MSE) may not be sufficiently low for the system to obtain adequate performance. A possible solution is to switch to a decision-directed (DD) adaptation which should be able to minimize the residual CMA steady state MSE [5]. However, as pointed out in [6], in order for such a transfer to be successful, the CMA steady state MSE should be sufficiently low. In practice, such a low level of MSE may not always be achievable by the CMA scheme.

Recently, De Castro and co-workers [6] have suggested an interesting solution to this problem. Rather than switching to a DD adaptation after the CMA has converged, they have proposed to operate a DD equalizer concurrently with a CMA equalizer. The weight adaptation of the DD equalizer follows that of the CMA equalizer and, to avoid error propagation due to incorrect decisions, the DD adjustment only takes place if the CMA adaptation is judged to have achieved a successful adjustment with high probability. At a small cost of slightly more than doubling the complexity of the very simple CMA, this concurrent CMA and DD equalizer is reported to obtain a dramatical improvement in equalization performance over the CMA [6]. Among various low-complexity blind equalization schemes for high-order QAM channels (e.g. [7]–[10]), this concurrent CMA and DD scheme represents a state-of-art technique. Another blind equalization scheme, which is relevant to the proposed concurrent CMA and soft decision-directed (SDD) blind equalizer, is the multi-stage blind clustering or a bootstrap maximum *a posteriori* probability (MAP) blind equalizer [11],[12].

The bootstrap MAP blind scheme was originally derived in [13] for the 4-QAM case and extended to M-QAM ($M > 4$) channels in [11],[12]. It is only slightly more complex than the CMA in terms of computational requirements per weight update, and has been shown to outperform the concurrent CMA and DD scheme, especially in terms of convergence rate [14],[15]. A drawback of this bootstrap MAP blind equalizer is that its adaptive process requires L-stage switchings, where $L = \log_2(M)/2$, and each stage of adaptation needs a different set of algorithm parameters. Thus, tuning of the bootstrap MAP algorithm is considerably more complicated than the concurrent CMA and DD scheme. The proposed concurrent CMA and SDD scheme may be viewed as operating a CMA equalizer and a last-stage bootstrap MAP equalizer concurrently. This concurrent CMA and SDD blind equalizer does not require complicated algorithm tuning and is computationally simpler than the concurrent CMA and DD scheme. Simulation results included demonstrate that both the concurrent CMA and DD scheme and the concurrent CMA and SDD scheme have the same steady-state equalization performance, but the latter has a faster convergence speed.

2 Low-complexity blind equalization

Consider the baseband model of a digital communication channel in which the received signal at symbol-spaced sample k is given by

$$r(k) = \sum_{i=0}^{n-1} a_i s(k-i) + e(k) \tag{1}$$

where n is the length of the channel impulse response (CIR), $a_i = a_{iR} + j a_{iI}$ are the complex-valued channel tap weights, $e(k) = e_R(k) + j e_I(k)$ is a complex-valued Gaussian white noise with $\mathrm{E}[e_R^2(k)] = \mathrm{E}[e_I^2(k)] = \sigma_e^2$ and $\mathrm{E}[\bullet]$ denoting expectation operator, and the complex-valued symbol sequence $s(k) = s_R(k) + j s_I(k)$ is assumed to be independently identically distributed and takes the value from the M-QAM symbol set defined by

$$\mathcal{S} = \{s_{il} = (2i - Q - 1) + j(2l - Q - 1), \;\; 1 \le i, l \le Q\} \tag{2}$$

with $Q = \sqrt{M} = 2^L$ and L being an integer. To remove the channel distortion, a symbol-spaced equalizer of the form

$$y(k) = \sum_{i=0}^{m-1} w_i r(k-i) = \mathbf{w}^T \mathbf{r}(k) \tag{3}$$

is employed, where m is the order of the equalizer, $\mathbf{w}(k) = [w_0 \; w_1 \cdots w_{m-1}]^T$ is the equalizer weight vector with $w_i = w_{iR} + j w_{iI}$, and $\mathbf{r}(k) = [r(k) \; r(k-1) \cdots r(k-m+1)]^T$ is the equalizer input vector. To deal with non-minimum phase channels, the equalizer should have a delay approximately $k_d \approx m/2$. Before blind adaptation, the equalizer weights are initialized to $w_i = 1 + j0$ for $i = k_d$ and $w_i = 0 + j0$ for $i \neq k_d$. It is recognized that a fractional-space equalizer can often achieve better performance. The purpose of this study is to assess a group of blind equalizers under a common framework. All the blind adaptive schemes studied here are equally applicable to fractional-space equalizers.

The constant modulus algorithm

The CMA adjusts the equalizer weights by minimizing the non-convex cost function

$$\bar{J}_{\mathrm{CMA}}(\mathbf{w}) = \mathrm{E}\left[\left(|y(k)|^2 - \Delta_2\right)^2\right] \tag{4}$$

using a stochastic gradient algorithm, where Δ_2 is a real positive constant defined by

$$\Delta_2 = \mathrm{E}\left[|s(k)|^4\right] / \mathrm{E}\left[|s(k)|^2\right] . \tag{5}$$

At sample k, given $y(k) = \mathbf{w}^T(k)\mathbf{r}(k)$, the CMA adapts $\mathbf{w}$ according to [1], [2]

$$\left.\begin{aligned} \epsilon(k) &= y(k)\left(\Delta_2 - |y(k)|^2\right) \\ \mathbf{w}(k+1) &= \mathbf{w}(k) + \mu\epsilon(k)\mathbf{r}^*(k) \end{aligned}\right\} \tag{6}$$

where μ is a small positive adaptive gain and $\mathbf{r}^*(k)$ is the complex conjugate of $\mathbf{r}(k)$. The CMA has a very simple computational complexity, as summarized in Table 1. Although M-QAM symbols do not fall on the circle of radius $\sqrt{\Delta_2}$, it is known that the cost function $\bar{J}_{\mathrm{CMA}}(\mathbf{w})$ is minimized at the equalizer weight solution which restores the signal constellation. Under certain conditions, the CMA converges to this solution subject to a possible phase shift.

The concurrent CMA and decision directed equalizer

De Castro and co-workers [6] proposed a blind equalization scheme that consists of a CMA equalizer and a DD equalizer operating concurrently. Specifically, let

$$\mathbf{w} = \mathbf{w}_c + \mathbf{w}_d. \tag{7}$$

Here $\mathbf{w}_c$ is the weight vector of the CMA equalizer which is designed to minimize the CMA cost function $\bar{J}_{\mathrm{CMA}}(\mathbf{w})$ by adapting $\mathbf{w}_c$ and $\mathbf{w}_d$ is the weight vector of the DD equalizer which is designed to minimize the decision based MSE

$$\bar{J}_{\mathrm{DD}}(\mathbf{w}) = \frac{1}{2}\mathrm{E}\left[|\mathcal{Q}[y(k)] - y(k)|^2\right] \tag{8}$$

by adjusting $\mathbf{w}_d$, where $\mathcal{Q}[y(k)]$ denotes the quantized equalizer output defined by

$$\mathcal{Q}[y(k)] = \arg\min_{s_{il}\in\mathcal{S}} |y(k) - s_{il}|^2. \tag{9}$$

More precisely, at sample k, given

$$y(k) = \mathbf{w}_c^T(k)\mathbf{r}(k) + \mathbf{w}_d^T(k)\mathbf{r}(k), \tag{10}$$

the CMA part adapts $\mathbf{w}_c$ according to the rule (6) by substituting $\mathbf{w}_c$ in the place of $\mathbf{w}$ with an adaptive gain μ_c. The DD adaptation follows immediately after the CMA adaptation but it only takes place if the CMA adjustment is viewed to be a successful one. Let

$$\tilde{y}(k) = \mathbf{w}_c^T(k+1)\mathbf{r}(k) + \mathbf{w}_d^T(k)\mathbf{r}(k)\,. \tag{11}$$

Then the DD part adjusts $\mathbf{w}_d$ according to [6]:

$$\mathbf{w}_d(k+1) = \mathbf{w}_d(k) + \mu_d \delta(\mathcal{Q}[\tilde{y}(k)] - \mathcal{Q}[y(k)])(\mathcal{Q}[y(k)] - y(k))\mathbf{r}^*(k) \tag{12}$$

where μ_d is the adaptive gain of the DD equalizer and the indicator function

$$\delta(x) = \begin{cases} 1, & x = 0 + j0, \\ 0, & x \neq 0 + j0. \end{cases} \tag{13}$$

It can be seen that $\mathbf{w}_d$ is updated only if the equalizer hard decisions before and after the CMA adaptation are the same. A potential problem of (hard) decision-directed adaptation is that if the decision is wrong, error propagation occurs which subsequently degrades equalizer adaptation. As analyzed in [6], if the equalizer hard decisions before and after the CMA adaptation are the same, the decision probably is a right one. The complexity of this concurrent CMA and DD blind equalizer, summarized in Table 1, is still linear in the equalizer order m. This concurrent blind equalizer does not suffer from a serious phase shift problem as the CMA does and is capable of lowering the steady state MSE, compared with the pure CMA.

The concurrent CMA and soft decision directed equalizer

After the equalization is accomplished, the equalizer output can approximately be expressed in two terms

$$y(k) \approx x(k) + v(k) \tag{14}$$

where $x(k) = s(k - k_d)$, k_d is an integer, and $v(k) = v_R(k) + jv_I(k)$ is approximately a Gaussian white noise. Thus, if the equalizer weights have correctly been chosen, the equalizer output can be modelled approximately by M Gaussian clusters with the cluster means being s_{il} for $0 \leq i, l \leq Q$. All the clusters have an approximate covariance

$$\begin{bmatrix} \mathrm{E}[v_R^2(k)] & \mathrm{E}[v_R(k)v_I(k)] \\ \mathrm{E}[v_I(k)v_R(k)] & \mathrm{E}[v_I^2(k)] \end{bmatrix} \approx \begin{bmatrix} \rho & 0 \\ 0 & \rho \end{bmatrix}. \tag{15}$$

Under the above conditions, the *a posteriori* probability density function (p.d.f.) of $y(k)$ is approximately

$$p(\mathbf{w}, y(k)) \approx \sum_{q=1}^{Q} \sum_{l=1}^{Q} \frac{p_{ql}}{2\pi\rho} \exp\left(-\frac{|y(k) - s_{ql}|^2}{2\rho}\right), \tag{16}$$

where p_{ql} are the *a priori* probabilities of s_{ql}, $1 \leq q, l \leq Q$, and they are all equal. Let the complex plane be divided into $M/4$ regular regions. As illustrated in Fig. 1, each region $S_{i,l}$ contains four symbol points

$$S_{i,l} = \{s_{pq},\ p = 2i-1, 2i, q = 2l-1, 2l\}. \tag{17}$$

If the equalizer output $y(k)$ is within the region $S_{i,l}$, a local approximation to the *a posteriori* p.d.f. of $y(k)$ is

$$\hat{p}(\mathbf{w}, y(k)) \approx \sum_{p=2i-1}^{2i} \sum_{q=2l-1}^{2l} \frac{1}{8\pi\rho} \exp\left(-\frac{|y(k) - s_{pq}|^2}{2\rho}\right) \tag{18}$$

where each *a priori* probability has been set to $\frac{1}{4}$.

The proposed scheme operates a CMA equalizer and a SDD equalizer concurrently. The CMA part is identical to that of the concurrent CMA and DD scheme. The SDD equalizer is designed to maximize log of the local *a posteriori* p.d.f. criterion

$$\bar{J}_{\mathrm{LMAP}}(\mathbf{w}) = \mathrm{E}[J_{\mathrm{LMAP}}(\mathbf{w}, y(k))] \tag{19}$$

by adjusting $\mathbf{w}_d$ using a stochastic gradient algorithm, where

$$J_{\mathrm{LMAP}}(\mathbf{w}, y(k)) = \rho \log\left(\hat{p}(\mathbf{w}, y(k))\right). \tag{20}$$

Specifically, the SDD equalizer adapts $\mathbf{w}_d$ according to

$$\mathbf{w}_d(k+1) = \mathbf{w}_d(k) + \mu_d \frac{\partial J_{\mathrm{LMAP}}(\mathbf{w}(k), y(k))}{\partial \mathbf{w}_d} \tag{21}$$

where

$$\frac{\partial J_{\mathrm{LMAP}}(\mathbf{w}, y(k))}{\partial \mathbf{w}_d} = \frac{\sum_{p=2i-1}^{2i} \sum_{q=2l-1}^{2l} \exp\left(-\frac{|y(k)-s_{pq}|^2}{2\rho}\right)(s_{pq} - y(k))}{\sum_{p=2i-1}^{2i} \sum_{q=2l-1}^{2l} \exp\left(-\frac{|y(k)-s_{pq}|^2}{2\rho}\right)} \mathbf{r}^*(k) \tag{22}$$

and μ_d is an adaptive gain. The choice of ρ should ensure a proper separation of the four clusters in $S_{i,l}$. If the value of ρ is too large, a desired degree of separation may not be achieved. On the other hand, if a too small ρ is used, the algorithm attempts to impose a very tight control in the size of clusters and may fail to do so. Apart from these two extreme cases, the performance of the algorithm does not critically depend on the value of ρ. As the minimum distance between the two neighbouring symbol points is 2, typically ρ is chosen to be less than 1.

Soft decision nature is evident in (22). Rather than commented to a single hard decision $\mathcal{Q}[y(k)]$ as the DD scheme does, alternative decisions are also considered in a local region $S_{i,l}$ that includes $\mathcal{Q}[y(k)]$, and each tentative decision is weighted by an exponential term $\exp(\bullet)$ which is a function of the distance between the equalizer soft output $y(k)$ and the tentative decision s_{pq}. This soft decision nature enables a simultaneous update of $\mathbf{w}_c$ and $\mathbf{w}_d$ without worrying error propagation and, therefore, simplifies the operation. It is also obvious that this SDD scheme corresponds to the last stage of the bootstrap MAP scheme given in [11],[12]. The complexity of the this concurrent CMA and SDD scheme is compared with those of the pure CMA scheme and the concurrent CMA and DD scheme of [6] in Table 1. The four $\exp(\bullet)$ evaluations can be implemented through look up table in practice. It can be seen that computational complexity per weight update of this proposed new scheme is simpler than that of the concurrent CMA and DD scheme.

3 Simulation study

The performance of the proposed low-complexity blind equalizer was compared with that of the concurrent CMA and DD one in a computer simulation using the standard CMA blind equalizer as a benchmark. Two performance criteria were used to assess the convergence rate of a blind equalizer. The first one was an estimated MSE at each adaptation sample based on a block of N_{MSE} data samples. The second one was the maximum distortion (MD) measure defined by

$$\mathrm{MD} = \frac{\sum_{i=0}^{n_c-1} |f_i| - |f_{i_{\max}}|}{|f_{i_{\max}}|} \tag{23}$$

where $\{f_i\}_{i=0}^{n_c-1}$ was the combined impulse response of the channel and equalizer, $n_c = n+m-1$ was the length of the combined impulse response, and

$$f_{i_{\max}} = \max\{f_i,\ 0 \le i \le n_c - 1\}. \tag{24}$$

The equalizer output signal constellation after convergence was also shown using $N_{\text{test}} = 6000$ testing data samples not used in adaptation. Two channels were used in evaluation, and their CIRs are given in Tables 2 and 3, respectively. In all the cases, a 23-tap equalizer was adopted. Table 4 lists the algorithm parameters used in the simulation for the three blind equalizers (μ for the CMA, μ_c and μ_d for the CMA+DD, and μ_c, μ_d and ρ for the CMA+SDD) together with the length of data samples N_{MSE} for estimating the MSE at each weight adaptation.

Example 1. In this example, 16-QAM symbols were transmitted through the 22-tap channel whose CIR is listed in Table 2. The noise power was set to $\sigma_e^2 = 0.0157$, giving rise to a channel signal to noise ratio (SNR) of 25 dB. The learning curves of the three blind equalizers, the CMA, the CMA+DD and the CMA+SDD, are compared in Fig. 2. The equalizer output signal constellations after convergence are shown in Fig. 3. It can be seen that both the concurrent CMA and SDD scheme and the concurrent CMA and DD scheme have the same steady-state performance, but the former has a faster convergence speed for this example.

Example 2. The transmitted data symbols were again 16-QAM, but the 5-tap channel given in Table 3 was used. The noise power was set to $\sigma_e^2 = 0.084$, corresponding to a SNR of 20 dB. The learning curves of the three blind equalizers, in terms of the estimated MSE and MD measure, are given in Fig. 4 (a) and (b), respectively. The three equalizer output signal constellations after convergence are shown in Fig. 5. Again, for this example, the two concurrent blind equalizers have the same steady-state performance, but the one with a SDD adaptation has a faster convergence speed.

Example 3. In this example, the transmitted data symbols were 64-QAM and the channel given in Table 2 was used. With a noise power of $\sigma_e^2 = 0.00209$, the SNR was 40 dB. The learning curves of the three blind equalizers, in terms of the estimated MSE and MD measure, are depicted in Fig. 6 (a) and (b), respectively. The equalizer output signal constellations after convergence are shown in Fig. 7. It can be seen that for this example the concurrent CMA and SDD scheme has a faster convergence rate than the concurrent CMA and DD scheme, and both blind equalizers have similar steady-state equalization performance.

Example 4. In this example, 64-QAM symbols were transmitted through the channel whose CIR is listed in Table 3. The noise power in the simulation was set to $\sigma_e^2 = 0.0354$, giving rise to a SNR of 30 dB. The learning curves of the three blind equalizers, in terms of the estimated MSE and MD measure, are depicted in Fig. 8 (a) and (b), respectively. The equalizer output signal constellations after convergence are illustrated in Fig. 9. This example again confirms that the proposed concurrent CMA and SDD scheme has a faster convergence rate than the concurrent CMA and DD scheme. It can also be seen that the two concurrent blind equalizers have similar steady-state equalization performance.

Example 5. The data constellation was 256-QAM and the 22-tap channel given in Table 2 was used in the simulation. The noise power was set to $\sigma_e^2 = 8.4 \times 10^{-7}$, giving rise to a SNR of 80 dB. The learning curves of the three blind equalizers, in terms of the estimated MSE and MD measure, are depicted in Fig. 10 (a) and (b), respectively. The equalizer output signal constellations after convergence are illustrated in Fig. 11. For this example, it is seen that the proposed new scheme converged marginally faster than the concurrent CMA and DD scheme, and the both concurrent blind equalizers have the same steady-state equalization performance.

Example 6. The data constellation was again 256-QAM but the 5-tap channel given in Table 3 was used in the simulation. With a noise power of $\sigma_e^2 = 1.43 \times 10^{-7}$, the SNR was 90 dB. The learning curves of the three blind equalizers, in terms of the estimated MSE and MD measure, are depicted in Fig. 12 (a) and (b), respectively, while the equalizer output signal constellations after convergence are illustrated in Fig. 13. For this example, faster convergence speed of the proposed new scheme over the concurrent CMA and DD scheme can clearly be seen. Again the both concurrent blind equalizers can be seen to have the same steady-state equalization performance.

4 Conclusions

In this paper, a novel low-complexity blind equalization scheme has been proposed based on operating a CMA equalizer and a SDD equalizer concurrently. Compared with a state-of-art low-complexity blind equalization scheme, namely the recently introduced concurrent CMA and DD blind equalizer, the proposed concurrent CMA and SDD blind equalizer has simpler computational requirements, faster convergence rate and identical steady-state equalization performance. This new blind equalizer, together with the concurrent CMA and DD blind equalizer, offer practical alternatives to blind equalization of higher-order QAM channels and provide significant equalization improvement over the standard CMA based blind equalizer.

References

[1] D. Godard, "Self-recovering equalization and carrier tracking in two-dimensional data communication systems," *IEEE Trans. Communications*, Vol.COM-28, pp.1867–1875, 1980.

[2] J.R. Treichler and B.G. Agee, "A new approach to multipath correction of constant modulus signals," *IEEE Trans. Acoustics, Speech and Signal Processing*, Vol.ASSP-31, No.2, pp.459–472, 1983.

[3] J.R. Treichler, "Application of blind equalization techniques to voiceband and RF modems," in *Preprints 4th IFAC Int. Symposium Adaptive Systems in Control and Signal Processing* (France), 1992, pp.705–713.

[4] N.K. Jablon, "Joint blind equalization, carrier recovery, and timing recovery for high-order QAM signal constellations," *IEEE Trans. Signal Processing*, Vol.40, No.6, 1383–1398, 1992.

[5] O. Macchi and E. Eweda, "Convergence analysis of self-adaptive equalizers," *IEEE Trans. Information Theory*, Vol.IT-3, No.2, pp.161–176, 1984.

[6] F.C.C. De Castro, M.C.F. De Castro and D.S. Arantes, "Concurrent blind deconvolution for channel equalization," in *Proc. ICC'2001* (Helsinki, Finland), June 11-15, 2001, Vol.2, pp.366–371.

[7] A. Benveniste and M. Goursat, "Blind equalizers," *IEEE Trans. Communications*, Vol.COM-32, pp.871–883, 1984.

[8] S. Bellini and F. Rocca, "Blind deconvolution: polyspectra or Bussgang techniques?" in *Digital Communications*, eds., E. Biglieri and G. Prati, North-Holland, Amsterdam, 1986, pp.251–263.

[9] G. Picchi and G. Prati, “Blind equalization and carrier recovering using a ‘stop-and-go’ decision directed algorithm,” *IEEE Trans. Communications*, Vol.COM-35, pp.877–887, 1987.

[10] S. Haykin, ed., *Blind Deconvolution*. Prentice Hall, Englewood Cliffs, NJ, 1994.

[11] S. Chen, S. McLaughlin, P.M. Grant and B. Mulgrew, “Reduced-complexity multi-stage blind clustering equaliser,” in *Proc. ICC’93* (Geneva, Switzerland), 1993, Vol.2, pp.1149–1153.

[12] S. Chen, S. McLaughlin, P.M. Grant and B. Mulgrew, “Multi-stage blind clustering equaliser,” *IEEE Trans. Communications*, Vol.43, No.3, pp.701–705, 1995.

[13] J. Karaoguz and S.H. Ardalan, “A soft decision-directed blind equalization algorithm applied to equalization of mobile communication channels,” in *Proc. ICC’92* (Chicago, U.S.A.), 1992, Vol.3, pp.343.4.1–343.4.5.

[14] S. Chen, T.B. Cook and L.C. Anderson, “Blind FIR equalisation for high-order QAM signalling,” to be presented at *6th Int. Conf. Signal Processing* (Beijing, China), Aug.26-30, 2002.

[15] S. Chen, T.B. Cook and L.C. Anderson, “A comparative study of two blind FIR equalizers,” submitted to *Digital Signal Processing*, 2001.

[16] S.C. Bateman and S.Y. Ameen, “Comparison of algorithms for use in adaptive adjustment of digital data receivers,” *IEE Proc. Pt.I*, Vol.137, No.2, pp.85–96, 1990.

Table 1: Comparison of computational complexity per weight update. The equalizer order is m.

equalizer	multiplications	additions	$\exp(\cdot)$ evaluations
CMA	$8 \times m + 6$	$8 \times m$	$-$
CMA+DD	$16 \times m + 8$	$20 \times m$	$-$
CMA+SDD	$12 \times m + 29$	$14 \times m + 21$	4

Table 2: A 22-tap channel impulse response from [16].

Tap No.	Real	Imaginary	Tap No.	Real	Imaginary
0	0.0145	-0.0006	11	0.0294	-0.0049
1	0.0750	0.0176	12	-0.0181	0.0032
2	0.3951	0.0033	13	0.0091	0.0003
3	0.7491	-0.1718	14	-0.0038	-0.0023
4	0.1951	0.0972	15	0.0019	0.0027
5	-0.2856	0.1896	16	-0.0018	-0.0014
6	0.0575	-0.2096	17	0.0006	0.0003
7	0.0655	0.1139	18	0.0005	0.0000
8	-0.0825	-0.0424	19	-0.0008	-0.0001
9	0.0623	0.0085	20	0.0000	-0.0002
10	-0.0438	0.0034	21	0.0001	0.0006

Table 3: A 5-tap channel impulse response.

Tap No.	Real	Imaginary
0	-0.2	0.3
1	-0.5	0.4
2	0.7	-0.6
3	0.4	0.3
4	0.2	0.1

Table 4: Algorithm parameter settings in simulation.

Example	N_{MSE}	CMA	CMA+DD		CMA+SDD		
		μ	μ_c	μ_d	μ_c	μ_d	ρ
1	250	10^{-5}	10^{-5}	0.0001	10^{-5}	0.001	0.6
2	250	10^{-5}	10^{-5}	0.0002	10^{-5}	0.0005	0.6
3	500	5×10^{-7}	5×10^{-7}	5×10^{-5}	5×10^{-7}	0.0002	0.6
4	500	2×10^{-7}	2×10^{-7}	5×10^{-5}	2×10^{-7}	0.0001	0.6
5	1000	2×10^{-8}	2×10^{-8}	5×10^{-5}	2×10^{-8}	5×10^{-5}	0.7
6	1000	10^{-8}	10^{-8}	2×10^{-5}	10^{-8}	3×10^{-5}	0.8

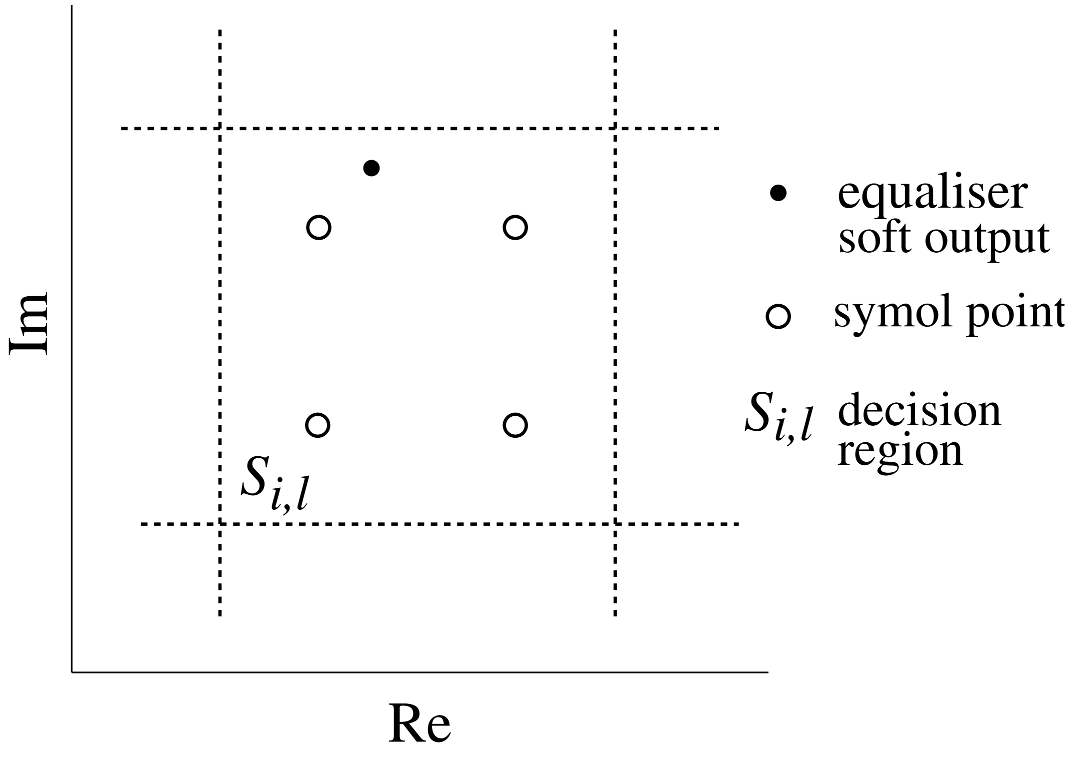

Figure 1: Illustration of local decision regions for soft decision-directed adaptation.

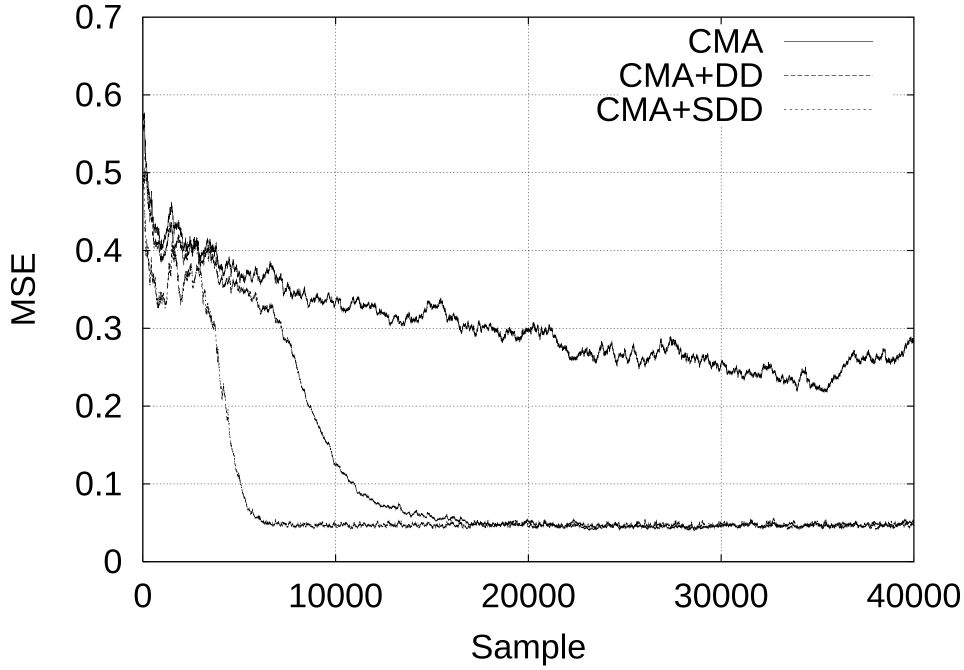

(a)

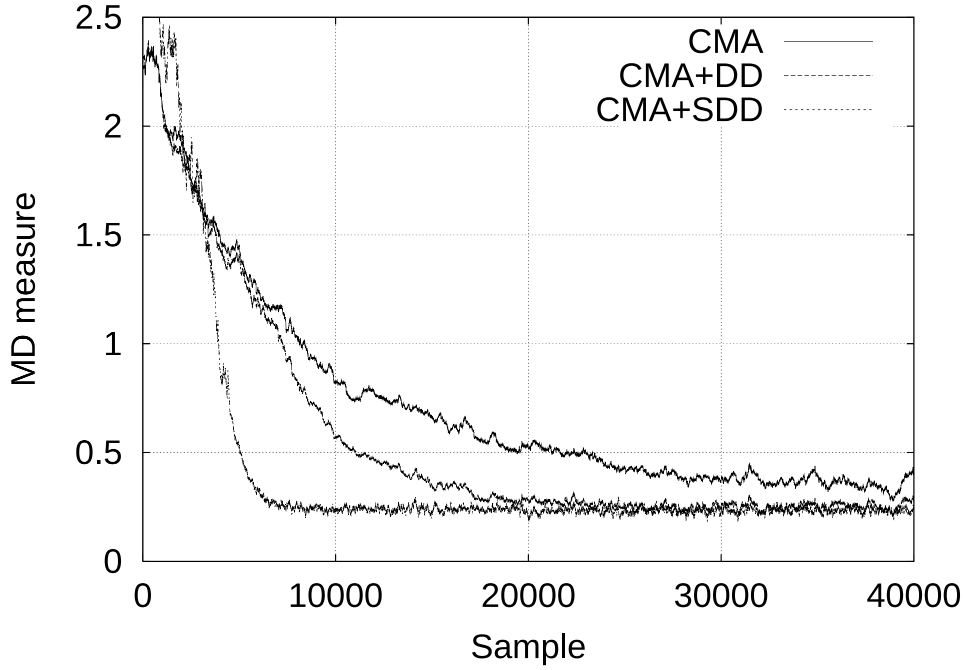

(b)

Figure 2: Comparison of convergence performance in terms of (a) estimated MSE and (b) MD measure for Example 1.

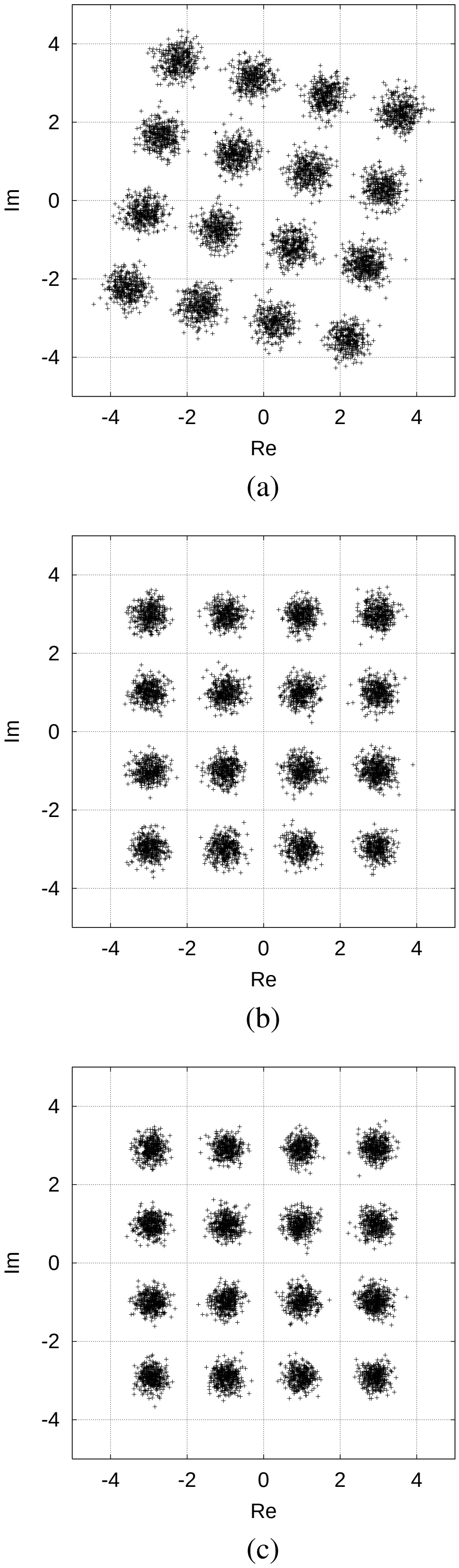

Figure 3: Equalizer output signal constellations after convergence (a) the CMA, (b) the CMA+DD, and (c) CMA+SDD for Example 1.

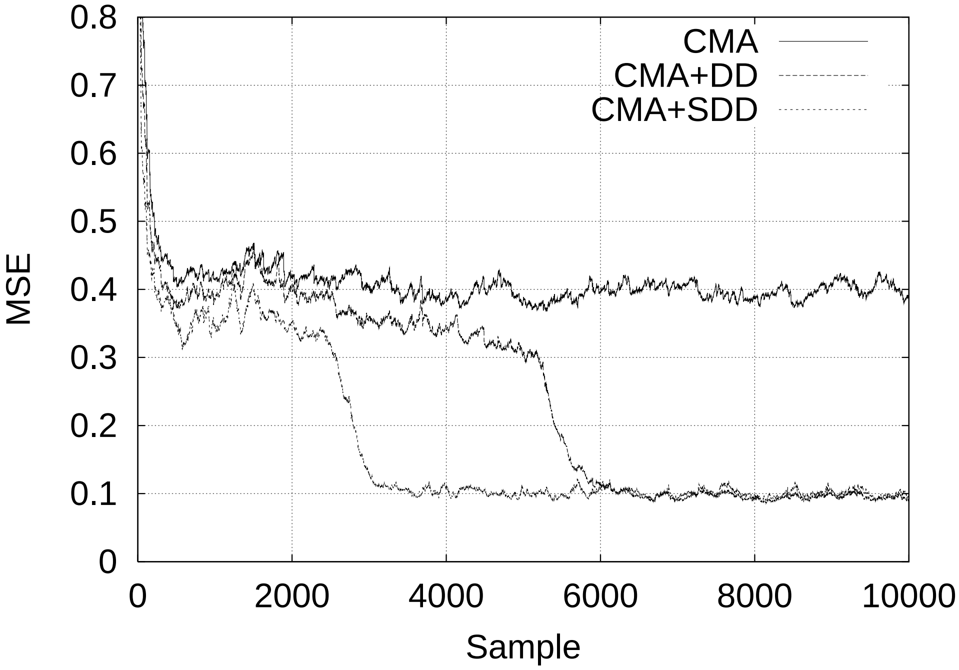

(a)

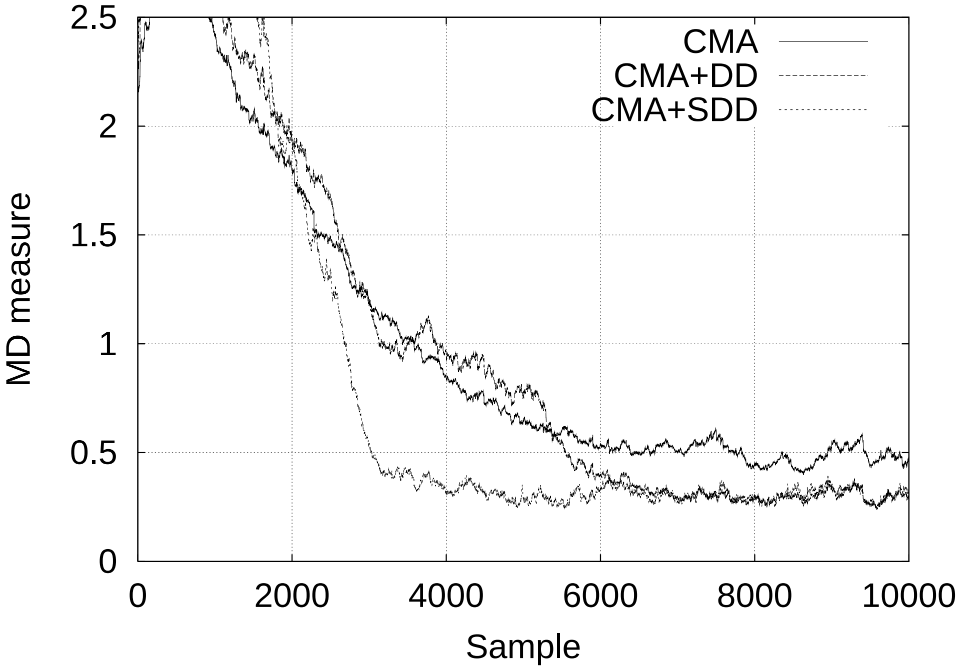

(b)

Figure 4: Comparison of convergence performance in terms of (a) estimated MSE and (b) MD measure for Example 2.

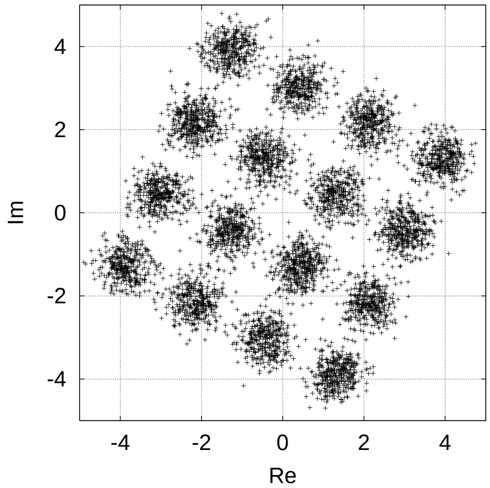

(a)

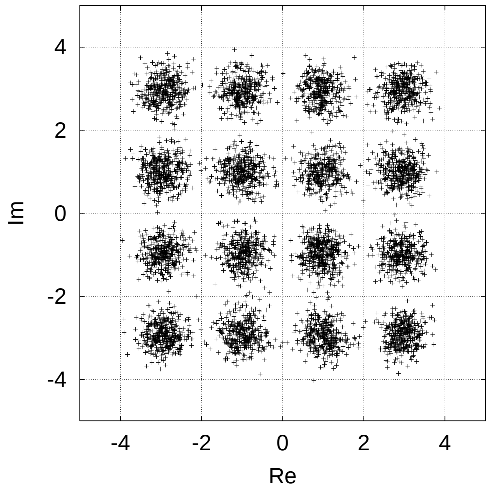

(b)

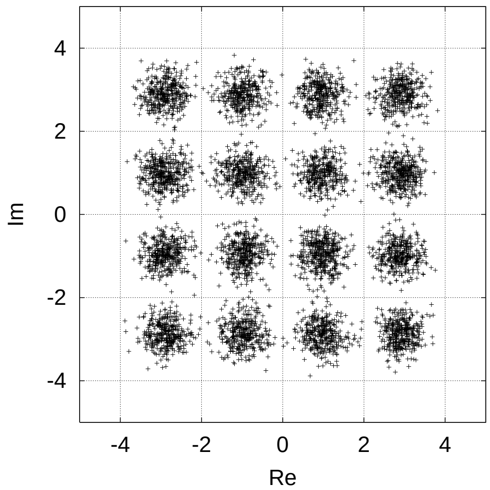

(c)

Figure 5: Equalizer output signal constellations after convergence (a) the CMA, (b) the CMA+DD, and (c) CMA+SDD for Example 2.

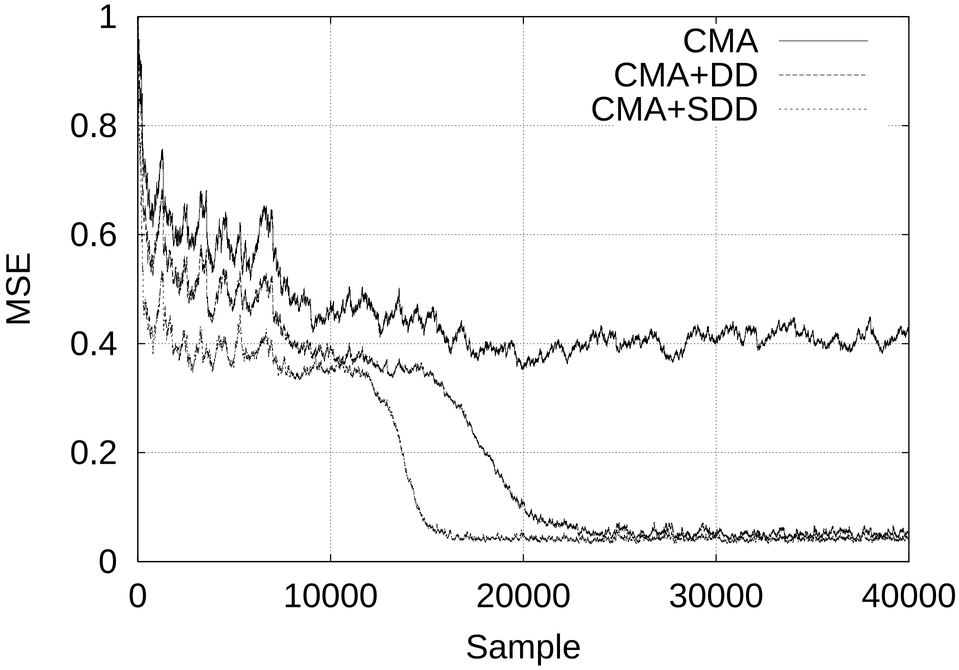

(a)

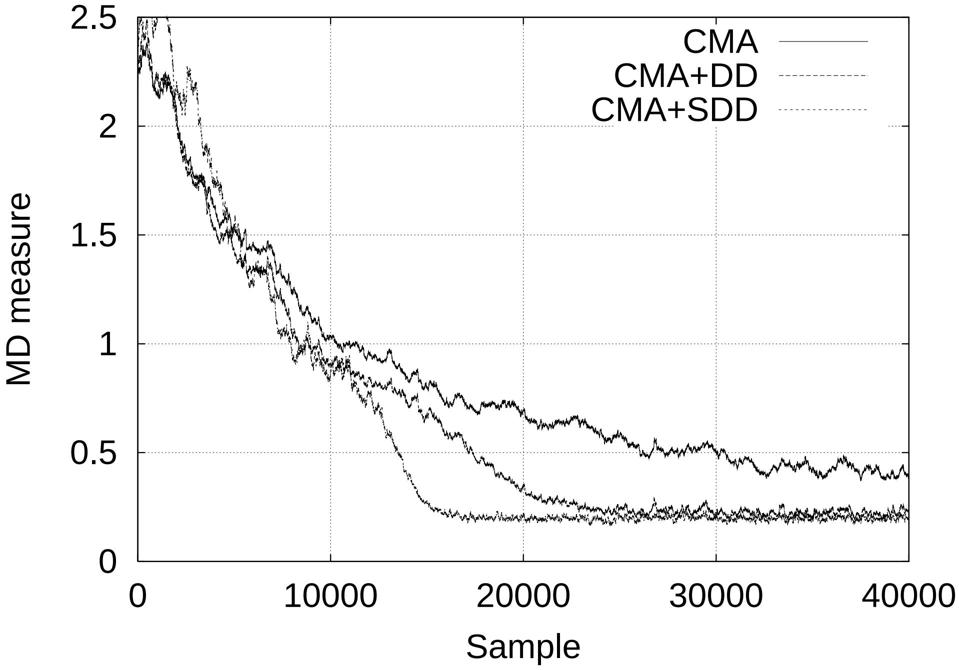

(b)

Figure 6: Comparison of convergence performance in terms of (a) estimated MSE and (b) MD measure for Example 3.

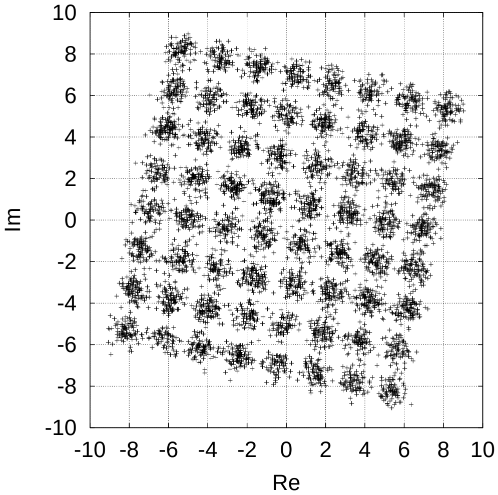

(a)

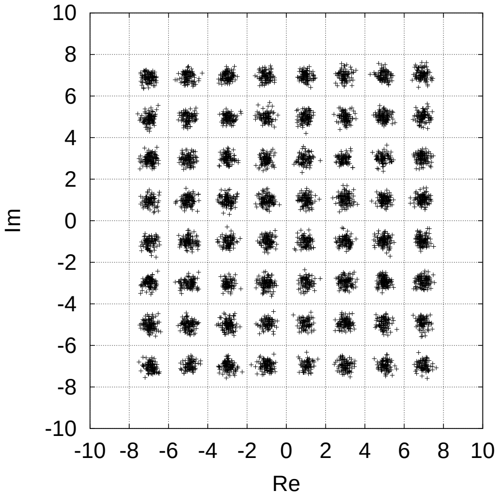

(b)

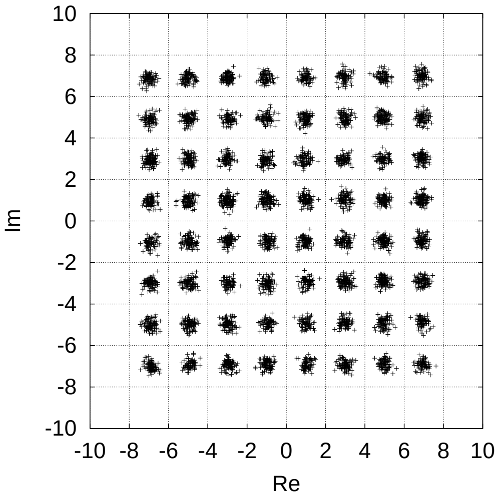

(c)

Figure 7: Equalizer output signal constellations after convergence (a) the CMA, (b) the CMA+DD, and (c) CMA+SDD for Example 3.

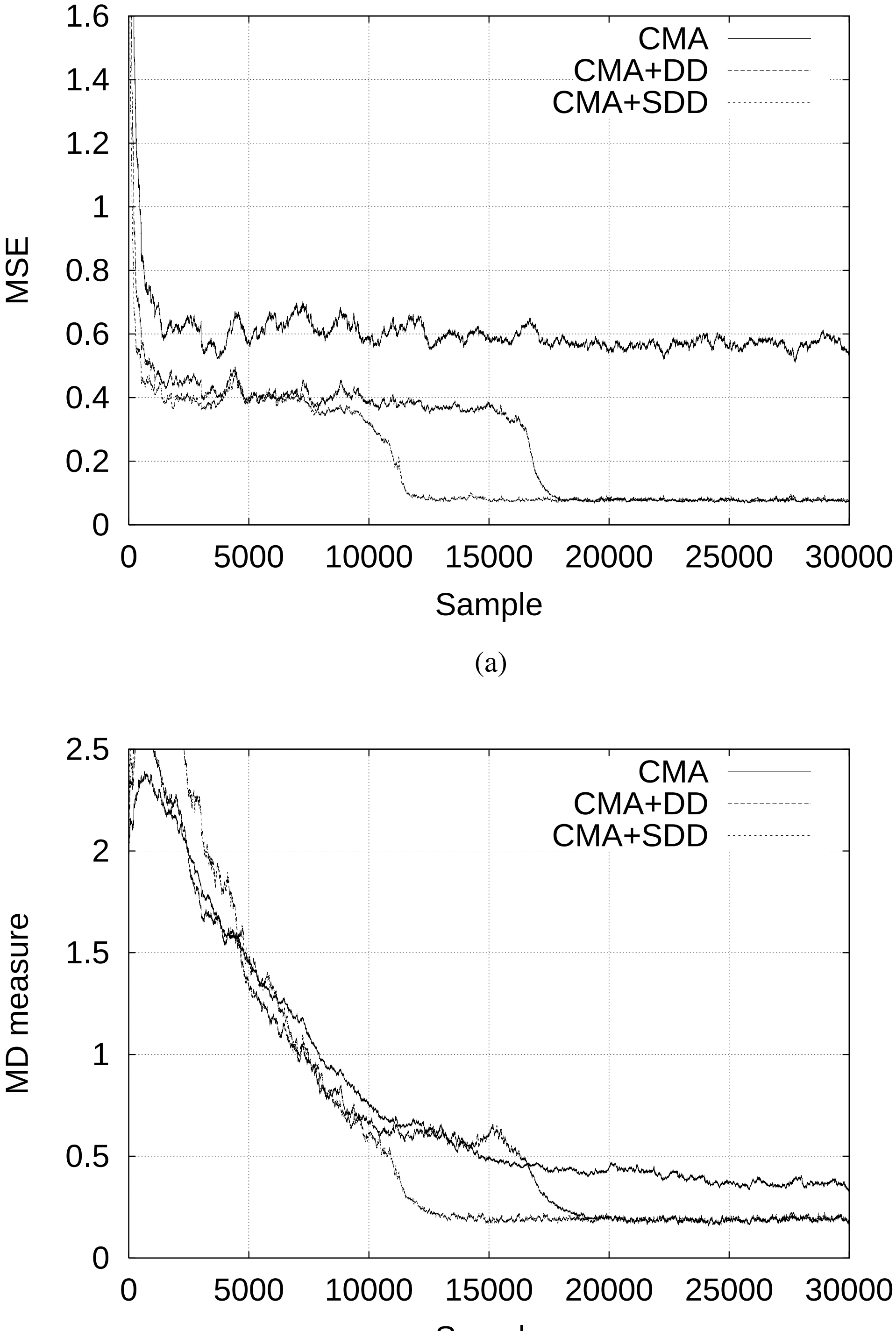

(a)

(b)

Figure 8: Comparison of convergence performance in terms of (a) estimated MSE and (b) MD measure for Example 4.

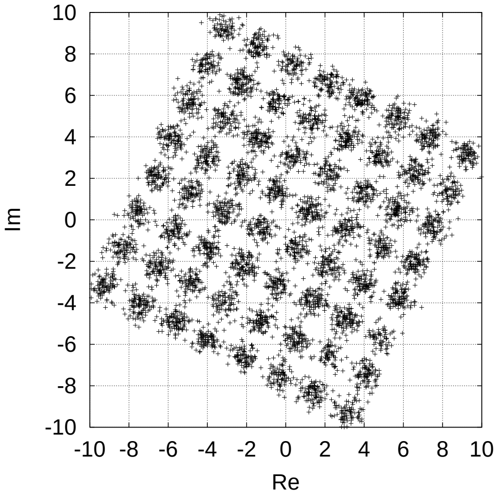

(a)

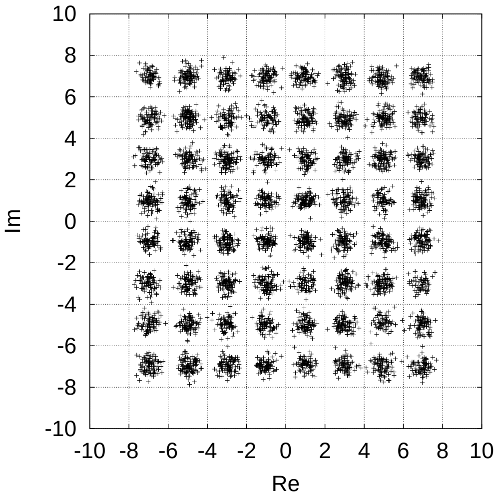

(b)

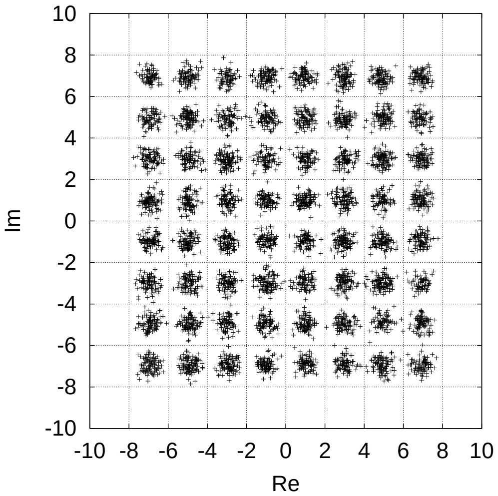

(c)

Figure 9: Equalizer output signal constellations after convergence (a) the CMA, (b) the CMA+DD, and (c) CMA+SDD for Example 4.

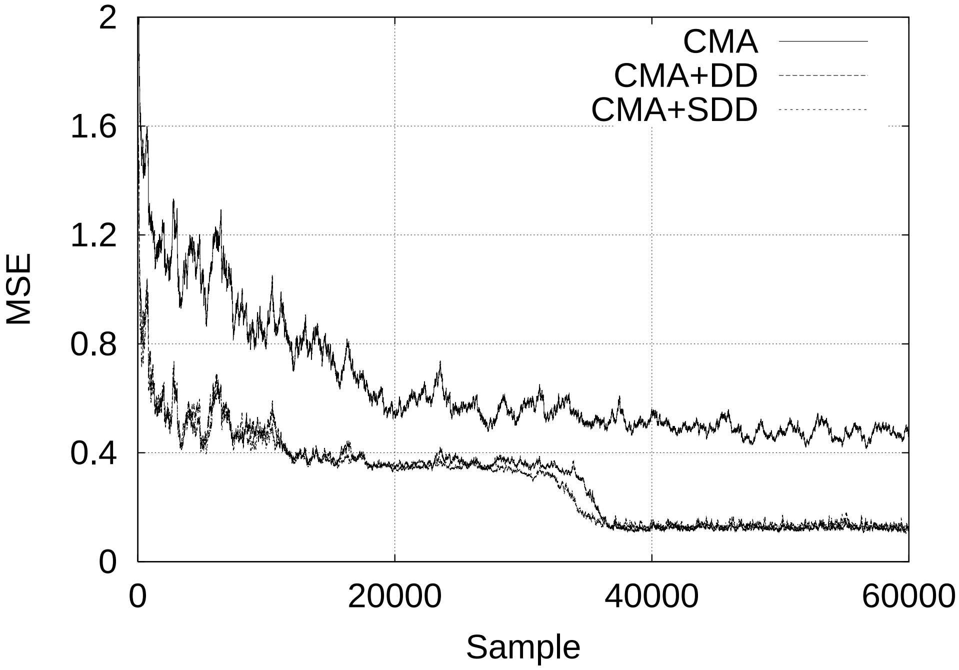

(a)

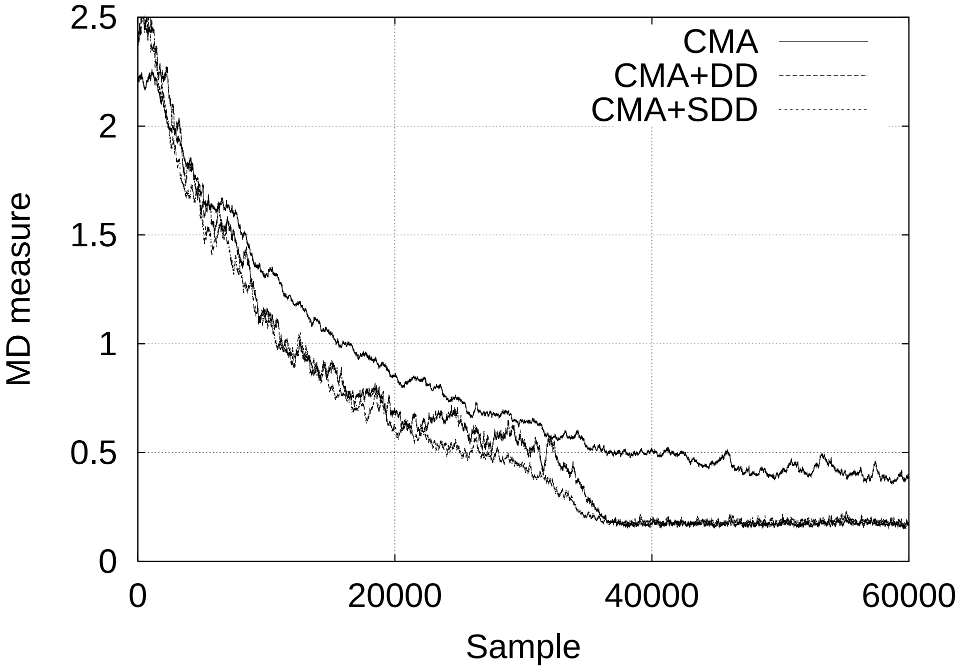

(b)

Figure 10: Comparison of convergence performance in terms of (a) estimated MSE and (b) MD measure for Example 5.

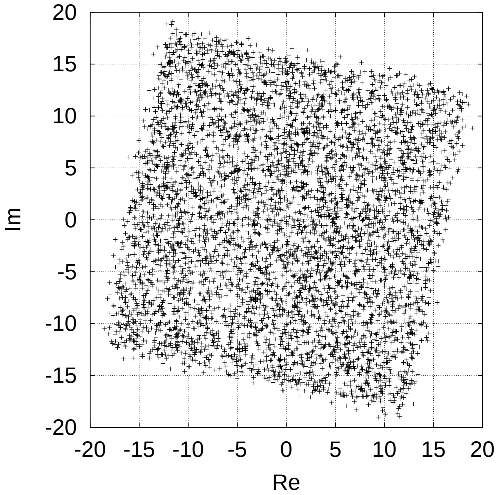

(a)

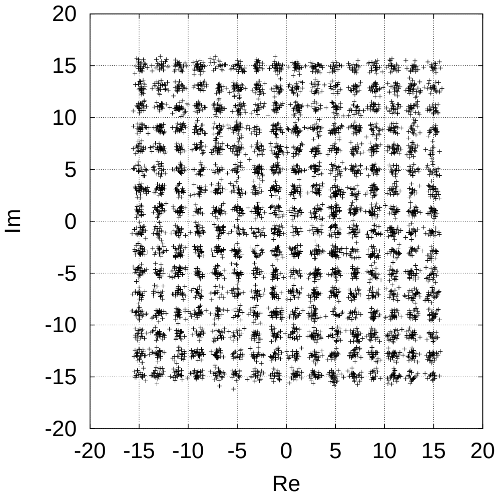

(b)

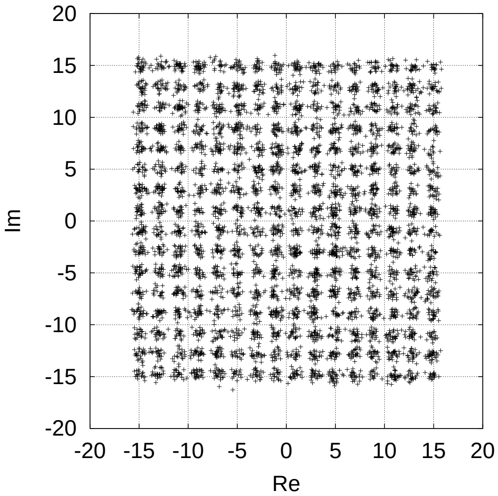

(c)

Figure 11: Equalizer output signal constellations after convergence (a) the CMA, (b) the CMA+DD, and (c) CMA+SDD for Example 5.

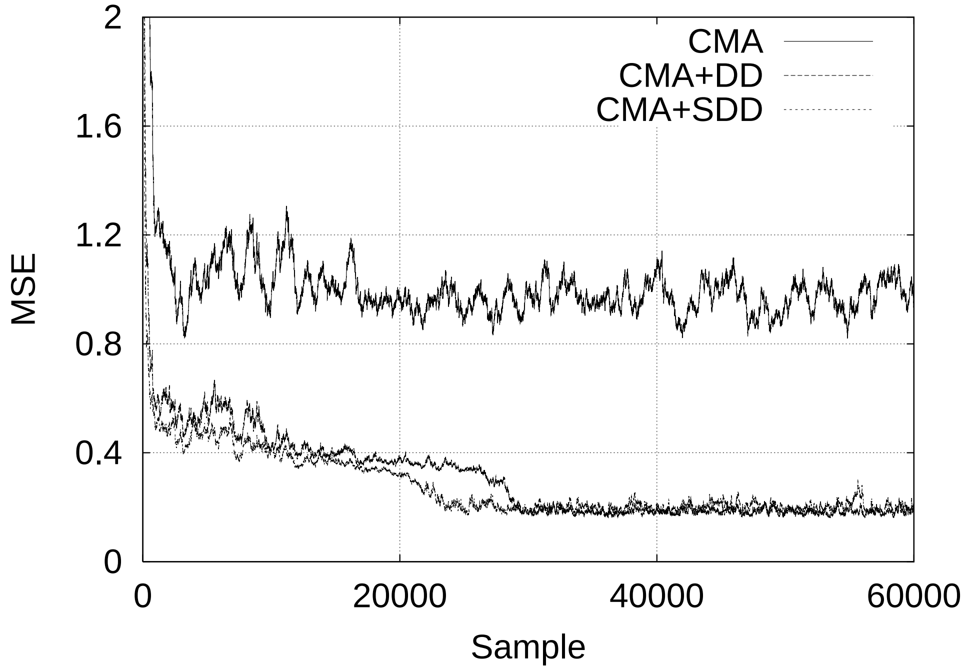

(a)

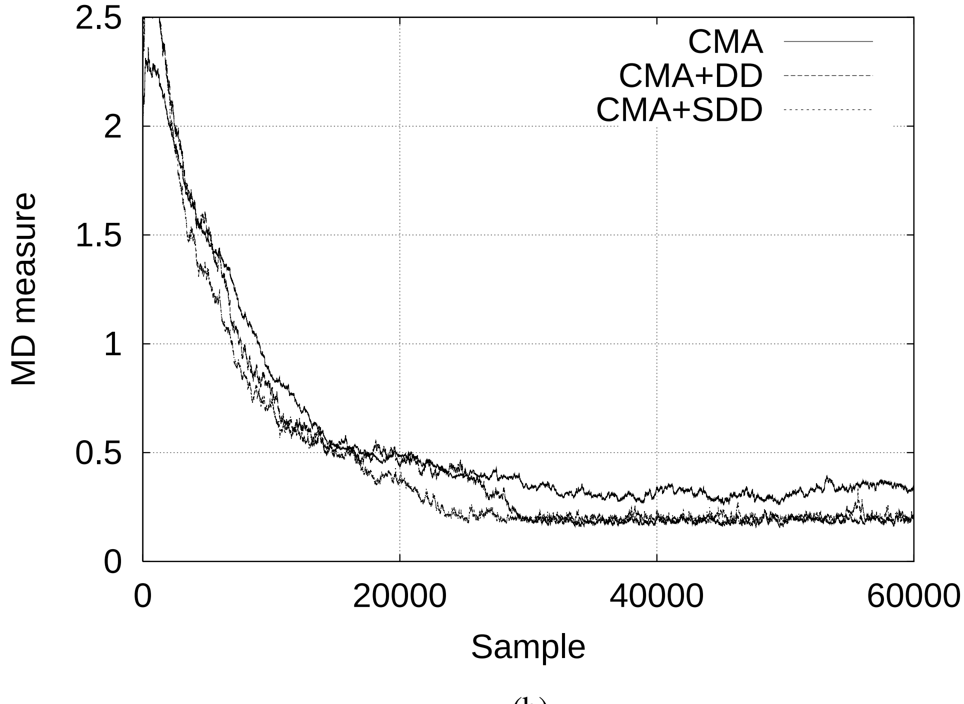

(b)

Figure 12: Comparison of convergence performance in terms of (a) estimated MSE and (b) MD measure for Example 6.

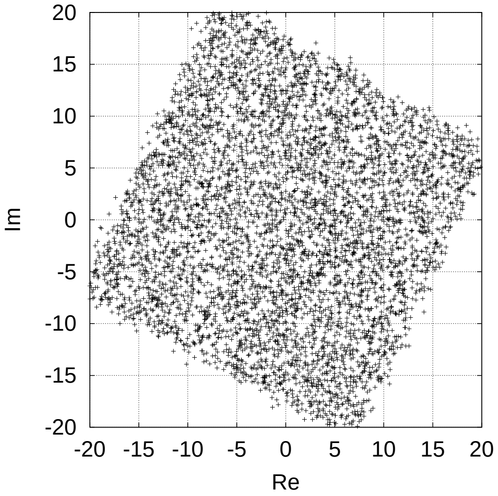

(a)

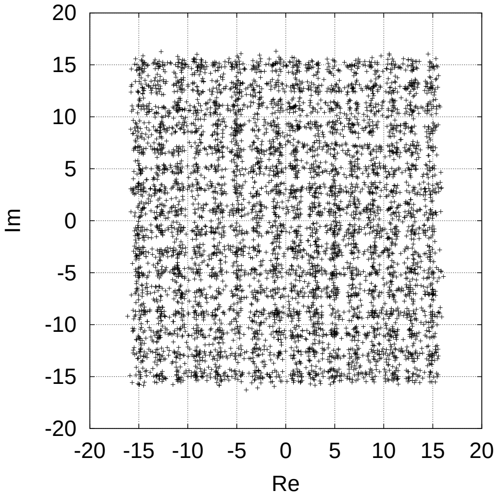

(b)

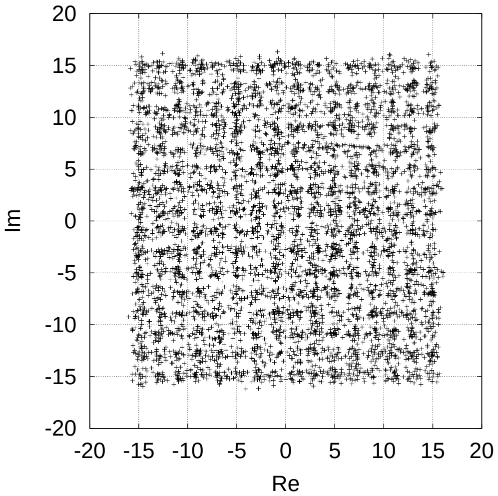

(c)

Figure 13: Equalizer output signal constellations after convergence (a) the CMA, (b) the CMA+DD, and (c) CMA+SDD for Example 6.